

## GLOBAL SCALE DEFORMATIONS CAUSED BY THE DART IMPACT: INSIGHTS TO THE COLLISIONAL EVOLUTION OF SMALL ASTEROIDS

S. D. Raducan<sup>1</sup>, M. Jutzi<sup>1</sup>. <sup>1</sup>Space Research and Planetary Sciences, Physikalisches Institut, University of Bern, Switzerland (E-mail: sabina.raducan@space.unibe.ch).

**Introduction:** NASA’s Double Asteroid Redirection Test (DART) mission will impact the smaller component of the 65803 Didymos asteroid system, Dimorphos, in late 2022 [1, 2]. The main goal of the mission is to alter the binary orbit period by an amount measurable from Earth [1]. A successful deflection of the Dimorphos will demonstrate the capabilities of the kinetic impact as an asteroid mitigation strategy. ESA’s Hera mission [2] will arrive at Dimorphos several years after the DART impact and will enable us to perform detailed characterisation of Dimorphos, including orbital and rotation states, surface properties, internal structure and composition. Moreover, the Hera mission will measure the crater volume and morphology resulted from the DART impact.

Past studies of the DART impact outcome [e.g., 3–5] have shown that the amount by which Dimorphos can be deflected is strongly dependant on its surface, subsurface and internal properties, and is non-unique –that is, impacting asteroids with different target properties and structures can result in the same deflection. However, [5] showed that such impacts can produce craters of different sizes and morphologies. Therefore, by measuring both  $\beta$  and the crater size and morphology, the predictive capabilities of numerical models can be validated and the asteroid deflection technique can be understood and ultimately reproduced. However, previous numerical models focused only on impacts on asteroid targets dominated by strength (from 100 Pa up to few MPa) and had relatively low cratering efficiencies. In these scenarios, the crater evolution spanned over only a few seconds after the impact.

Recent results of the SCI impact on Ryugu [6] inferred that at least the near-surface of the asteroid may not be dominated by strength, which, in turn, suggests that cratering is controlled to a large extent by gravity despite its very low value. These findings might also be applicable to Dimorphos. Studies by [7] found that certain impacts with large enough critical specific impact energies,  $Q_{crit}$ , do not produce impact craters but instead can cause global deformation of the target. Figure 1 shows  $Q_{crit}$  as a function of impact velocity for which such events are expected to occur. The scaling relations found by [7] only apply to impacts into comet-like bodies and the objects studied were significantly larger than Dimorphos. However, it is possible that the DART impact, which will have  $Q_{crit} \approx 2.5 J/kg$ , might also produce global scale effects.

The aim of this work is to numerically simulate DART-like impacts on asteroids that use realistic material models

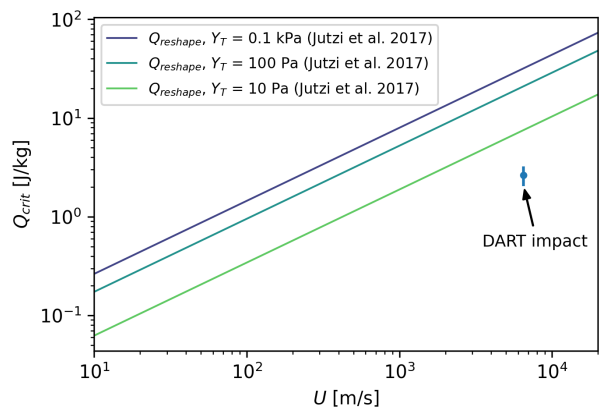


Figure 1: Critical specific impact energies,  $Q_{reshape}$ , as a function of impact velocity. The solid lines are showing the scaling  $Q_{reshape}$  that cause target deformation. The scaling relations were found by [7] for shape-changing collisions on generic bi-lobe shapes ( $\approx 5$  km in diameter), with  $Y_T = 10$  Pa, 100 Pa and 1 kPa. The DART mission impact ( $Q_{crit} \approx 2.5 J/kg$ ) is plotted for comparison.

and evaluate the resulting crater morphologies and possible target shape deformations.

**Numerical Model:** Here we use Bern’s parallel Smooth Particle Hydrodynamics (SPH) impact code [8, 9] to model the DART impact scenario on Dimorphos-like spherical asteroid targets and track the evolution of the target for up to 2 hours after the impact. The target was modelled using the Tillotson equation of state (EoS) for basalt [10]. Numerical models of impacts into low strength-low gravity regimes are computationally expensive and therefore challenging to model. In order to track the long evolution of the target, here we define impact scenario that allows for faster calculation times. This was achieved by choosing a target material with a low elastic wave speed of  $\approx 250$  m/s, which is typical for low-strength, porous materials. We describe the material strength with a pressure-dependent strength model [11], for which we systematically varied the shear strength at zero pressure,  $Y_0$  (between 0 Pa (no cohesion) and 50 Pa) and the coefficient of internal friction,  $f$  (between 0.4 and 1.2). The initial target porosity was kept constant at 40% and was modelled using the  $P - \alpha$  model [8] with a relatively low crushing strength (10 MPa). Due to the very long timescale required to see the effects of the DART impact, the simulations had a limited resolution of  $5 \times 10^5$  SPH particles. The impact velocity was set to 6 km/s. The models used

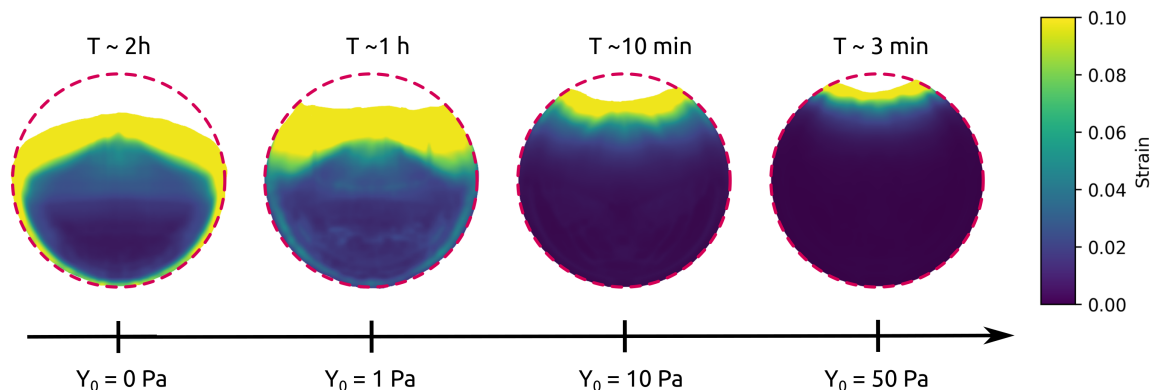


Figure 2: Two-dimensional slices through SPH simulations of DART-like impacts on 150 m spherical bodies.

self gravity, which was re-calculated every few time steps.

### Results and discussion:

**Crater morphology:** The size and morphology of the DART crater is of paramount importance for determining the asteroid's near-surface properties and structure. Figure 2 shows cross-sections through SPH simulations of DART-like impacts into spherical targets with varying initial cohesion ( $Y_0 = 0\text{--}50$  Pa). For scenarios with  $Y_0 \gtrsim 0$  Pa, the target cohesion is the dominant force that stops the crater cavity from growing. Therefore, with decreasing target cohesion, more material is displaced and gets ejected above escape speed. While impacts into targets stronger than  $Y_0 \approx 10$  Pa create well defined bowl-shaped craters, impacts into weaker targets create morphologies that do not resemble an impact crater anymore. For these scenarios ( $Y_0 < \approx 10$  Pa) the curvature of the target also plays a major role.

**Displaced mass ( $M_{dis}$ ):** For  $Y_0 > 10$  Pa impact scenarios, most of the material gets excavated from the crater with velocities larger than the escape velocity ( $M_{dis} \approx M_{esc}$ , where  $M_{esc}$  is the mass escaping the system). On the other hand, when  $Y_0 < 10$  Pa,  $M_{dis} \gg M_{esc}$  (Table 1). These impact scenarios occur in the sub-catastrophic collision regime, a regime between cratering and catastrophic collisions [e.g. 12]. In these cases, there is a relatively small fraction of the target material that escapes the target, but instead there is significant material re-distribution, leading to a change of the overall shape. Large shape deformations of Dimorphos are expected to affect the mutual orbit period, which is a critical parameter for calculating the kinetic impact deflection [13].

**Conclusions and future work:** The DART impact on cohesionless spherical bodies is likely to produce morphologies that are dissimilar to cratering and change the global morphology of the asteroid. Our modelling results together with the future observations by the Hera mission

Table 1: Summary of ejected mass above escape velocity ( $M_{esc}(> v_{esc})$ ) and mass excavated below escape velocity ( $M_{dis}(< v_{esc})$ ), where  $v_{esc} = 9$  cm/s.

$Y_0$ (Pa)	$M_{esc}/M_t$ (%)	$M_{dis}/M_t$ (%)
0	1.18	6.14
1	0.94	2.41
10	0.54	0.93
50	0.31	0.38

will therefore provide constraints regarding the evolution of the shapes and structures of small asteroids by sub-catastrophic impacts.

However, these low-strength low-gravity regime impacts are challenging to model and only limited number of impact scenarios have been studied so far. Future work aims to explore the effects of initial target shape, structure and impact geometry. In parallel, coupled SPH/N-body will be applied to investigate the long-term evolution and deposition of low-velocity ejecta [14].

**Acknowledgements:** This work has received funding from the European Union's Horizon 2020 research and innovation programme under grant agreement No. 870377.

**References:** [1] Cheng, A. F. et al. (2018) *Planet. Space Sci.*, 157:104–115. [2] Michel, P. et al. (2018) *Adv Space Res.* 62:2261–2272. [3] Jutzi, M. & Michel, P. (2014) *Icarus*, 229:247–253. [4] Raducan, S. D. et al. (2019) *Icarus*, 329:282–295. [5] Raducan, S. D. et al. (2020) *Planet. Space Sci.*, 180:104756. [6] Arakawa, M. et al. (2020) *Science*, 368:67–71. [7] Jutzi, M. et al. (2017) *A&A*, 597:A61. [8] Jutzi, M. et al. (2008) *Icarus*, 198:242–255. [9] Jutzi, M. (2015) *Planet. Space Sci.*, 107:3–9. [10] Benz, W. & Asphaug, E. (1999) *Icarus*, 142:5–20. [11] Collins, G. S. et al. (2004) *Meteorit. Planet. Sci.*, 39:217–231. [12] Jutzi, M. (2019) *Planet. Space Sci.* 177:104695. [13] Hirabayashi, M. et al. (2019) *Adv. Space Res.*, 63:2515–2534. [14] Zhang, Y. (2021) *LPSC LII*,